GENERALIZED SCATTERING MATRIX OF WAVEGUIDE CORNERS DISTORTED BY DISCONTINUITIES IN THE RESONATOR REGION

Vladimir A. Labay and Jens Bornemann

Laboratory for Lightwave Electronics, Microwaves and Communications (LLiMiC)
Department of Electrical and Computer Engineering
University of Victoria, Victoria B.C. Canada V8W 3P6

ABSTRACT

A new generalized scattering matrix formulation is presented for the calculation of waveguide corners distorted by discontinuities. The novel approach lies in the fact that the introduction of shorting planes some distance away from the actual discontinuity - as is common practise in analyses known so far - is entirely avoided. Therefore, this method allows the computation of components in which other structures are connected as closely as possible to the waveguide corner. This follows directly from the rigorous incorporation of higher-order mode interactions. Previously, only fundamental-mode scattering parameters could be calculated and, therefore, connected components had to be far enough away from the waveguide corner in order to avoid interference of reactive fields.

Consequently, the theory presented in this paper will, first, allow the calculation and design of more complex waveguide components and, secondly, contribute to a more efficient use of component space. At the examples of 90- and 180-degree waveguide bends, the theoretical model is compared with measurements and a finite-element analysis. Results are found to be in good agreement.

I. INTRODUCTION

Waveguide corners [1] and T-junctions [2] form integral parts in the design and realization of waveguide components and systems, e.g. [3]. In order to fully incorporate the electrical properties of such structures in a computer-aided design routine, their generalized scattering matrix must be known. This allows to account for higher-order mode interactions with connected components [2, 3]. For the waveguide corner, a resonator model based on mode-matching techniques [1] is applicable as long as the so-called resonator region can be represented by well-known rectangular cavity functions. This method can also be used to simulate low-return-loss mitered corners by reducing the actual resonator region in size and adding matching discontinuities outside the resonator region, i.e., in the connected waveguide arms [4]. However, such an approach increases the distance between the corner and following circuitry and, therefore, is often undesirable for its additional space requirements.

Alternatively, discontinuities can be placed directly into the resonator region in order to obtain lower return loss of the corner (Fig. 1). However, the eigenfunctions of the resonator region are not known in such a case. One approach to model a resonator region with built-in discontinuities is to computationally conduct resonator experiments by placing shorts some distance away from the actual waveguide corner [5, 6]. However, the resulting overall scattering parameters show nonlinear dependence on the matrices obtained by the resonator experiments (e.g., input reflection coefficient matrices). Consequently, only the fundamental-mode scattering matrix of the entire waveguide corner (or T-junction) can be extracted (c.f. [4], "These [shorting] planes are located far enough so as not to perturb the reactive fields in the proximity of the discontinuity.") In other words, if following circuitry is connected at a smaller distance, i.e. higher-order modes interact, then the analysis is invalid.

Therefore, this paper presents a technique which allows the entire generalized or modal scattering matrix of a discontinuity-distorted waveguide corner to be calculated without any restrictions for components connected to the corner. The technique is based on the rigorous field-theory treatment of the discontinuities within the resonator region and the complete matching conditions at the corner interfaces.

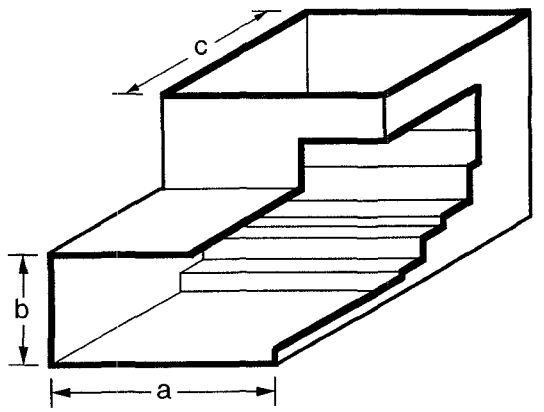

Fig. 1 Corner in rectangular waveguide with discontinuities in the resonator region.

II. THEORY

Fig. 2 shows the division of the N-1 stepped waveguide corner into N subregions with respect to z- (subregions $IIIa_{1...N}$) as well as y- (subregions $IIIb_{1...N}$) directions. In regions $i \in [I, IIIa]$, the electromagnetic field is given by

$$\vec{E}^i = [(\hat{u}_z \times \nabla_z T^i_{Eq}), \left(-\nabla_z T^i_{Mp} \pm \frac{(k^i_{cMp})^2}{jk^i_{zMp}} \hat{u}_z T^i_{Mp}\right)]$$

$$\bullet \, \mathrm{Diag}\{\sqrt{Z^i_{Eq,\,Mp}}\, \exp(\mp jk^i_{zEq,\,Mp} z)\} \begin{bmatrix} A^i_{Eq} + B^i_{Eq} \\ A^i_{Mp} + B^i_{Mp} \end{bmatrix} \quad (1)$$

$$\vec{H}^i = [\left(-\nabla_z T^i_{Eq} \pm \frac{(k^i_{cEq})^2}{jk^i_{zEq}} \hat{u}_z T^i_{Eq}\right), (-\hat{u}_z \times \nabla_z T^i_{Mp})]$$

$$\bullet \, \mathrm{Diag}\{\sqrt{Y^i_{Eq,\,Mp}}\, \exp(\mp jk^i_{zEq,\,Mp} z)\} \begin{bmatrix} A^i_{Eq} - B^i_{Eq} \\ A^i_{Mp} - B^i_{Mp} \end{bmatrix} \quad (2)$$

with well-known immittances $Z^i_{Eq,Mp}$, $Y^i_{Eq,Mp}$, wavenumbers $k^i_{zEq,Mp}$, wave amplitudes $A^i_{Eq,Mp}$, $B^i_{Eq,Mp}$ and cross-section functions

$$T^i_{Eq}(x,y) = A^i_{mn} \frac{\cos\left[\frac{m\pi}{a_i}(x - x_{oi})\right]}{\sqrt{1+\delta_{0m}}} \bullet \frac{\cos\left[\frac{n\pi}{b_i}(y - y_{oi})\right]}{\sqrt{1+\delta_{0n}}} \quad (3)$$

$$T^i_{Mp}(x,y) = D^i_{mn} \sin\left[\frac{m\pi}{a_i}(x - x_{oi})\right] \sin\left[\frac{n\pi}{b_i}(y - y_{oi})\right] \quad (4)$$

(For details, the reader is referred to [3].) Note that TE (index q) and TM (index p) modes are ordered with respect to sequences (m,n) of increasing cutoff frequencies. The expressions in regions $i \in [\mathrm{II}, \mathrm{IIIb}]$ are similar once the shift in coordinates and the change in propagation directions are incorporated.

As shown in Fig. 2, the electric fields within the subregions $\mathrm{IIIa}_{1\ldots N}$ and $\mathrm{IIIb}_{1\ldots N}$ are matched, first, by assuming electric walls at the respective other port. The fields within the subregions can then be represented as

$$E^{\mathrm{IIIa}_n}, H^{\mathrm{IIIa}_n} = f(\underline{A}^{\mathrm{IIIa}_1}, \mathbf{S}^{\mathrm{IIIa}_{1\ldots N}}_{i,k}) \quad (5)$$

$$E^{\mathrm{IIIb}_n}, H^{\mathrm{IIIb}_n} = f(\underline{A}^{\mathrm{IIIb}_N}, \mathbf{S}^{\mathrm{IIIb}_{N\ldots 1}}_{i,k}) \quad (6)$$

where vectors $\underline{A}$ hold the amplitude coefficients of the two subregions (IIIa_1 and IIIb_N), which directly interface with the waveguide ports I and II, and $\mathbf{S}_{i,k}$ (i,k=1,2) are the generalized two-port scattering matrices of the individual discontinuities within the corner region. The expressions (3) and (4) can now be used to satisfy the matching conditions at the two cross-sections interfacing the corner region III with waveguide port I at z=0

$$E^I_{x,y} = E^{\mathrm{IIIa}_1}_{x,y} \quad (7)$$

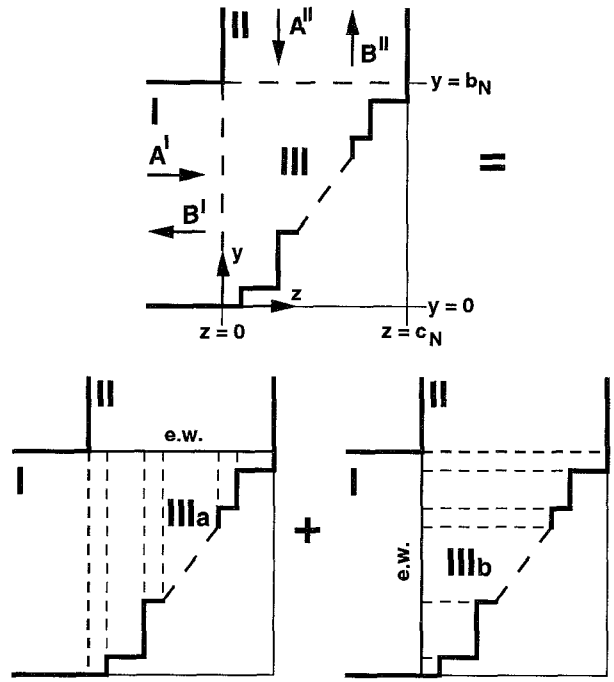

Fig. 2 Superposition of subregions for field-theory treatment.

$$H^I_{x,y} = H^{\mathrm{IIIa}_1}_{x,y} + \sum_{n=1}^{N} H^{\mathrm{IIIb}_n}_{x,y} \quad (8)$$

and with waveguide port II at $y=b_N$

$$E^{\mathrm{II}}_{x,z} = E^{\mathrm{IIIb}_N}_{x,z} \quad (9)$$

$$H^{\mathrm{II}}_{x,z} = H^{\mathrm{IIIb}_N}_{x,z} + \sum_{n=1}^{N} H^{\mathrm{IIIa}_n}_{x,z} \quad (10)$$

With matching conditions (7) and (9), wave amplitudes $\underline{A}^{\mathrm{IIIa}_1}$, $\underline{A}^{\mathrm{IIIb}_N}$ (c.f. (5), (6)) can be expressed by $\underline{A}^{\mathrm{I}}$, $\underline{B}^{\mathrm{I}}$, $\underline{A}^{\mathrm{II}}$ and $\underline{B}^{\mathrm{II}}$, which are finally rearranged in (6) and (8) to form the generalized scattering matrix of the waveguide corner of Fig. 1.

$$\begin{bmatrix} \underline{B}^I_{Eq} \\ \underline{B}^I_{Mp} \\ \underline{B}^{II}_{Eq} \\ \underline{B}^{II}_{Mp} \end{bmatrix} = [S] \begin{bmatrix} \underline{A}^I_{Eq} \\ \underline{A}^I_{Mp} \\ \underline{A}^{II}_{Eq} \\ \underline{A}^{II}_{Mp} \end{bmatrix} \quad (11)$$

With 25 modes and a five-step approximation of the miter, the calculation of the entire generalized scattering matrix takes about one minute per frequency point on a IBM RISC 6000/530 workstation.

III. RESULTS

A convergence analysis of an E-plane corner assuming a staircase approximation of the mitered structure of [7] is presented in Figs. 3. Good agreement with the results of [7] is obtained for 12 steps. A similar investigation regarding the number of modes for a constant number of steps reveals that the consideration of 20 to 25 modes in the theoretical model is sufficient. Fig. 3a shows the results for a TE_{10}-mode (E-plane) excitation. The resonance effect around 9 GHz is frequently encountered (and measured) in E-plane square waveguide applications to appear slightly below TE_{11}- mode cutoff, e.g. [8].

For the H-plane (TE_{10}-mode excitation) in Fig. 3b, such resonances do not occur due to the vanishing electric field tangential to the miter boundary. However, this case requires a higher number of modes (up to 35) to satisfy this boundary condition and, additionally, more steps (e.g. 15) to approximate the plane miter used in [7]. The differences in this figure between our results and those presented in [7] can clearly be attributed to this fact since the stepped corner will always exhibit a higher frequency dependence than the plane miter.

As pointed out in [7], a change in the miter dimension enables also the H-plane return loss to peak within the fundamental-mode frequency range of the two orthogonal polarizations. This is demonstrated in Fig. 4, showing again good agreement with the data provided in [7].

The advantage of this model, which calculates the generalized or modal scattering matrix of the discontinuity-perturbed waveguide corner instead of only its fundamental-mode

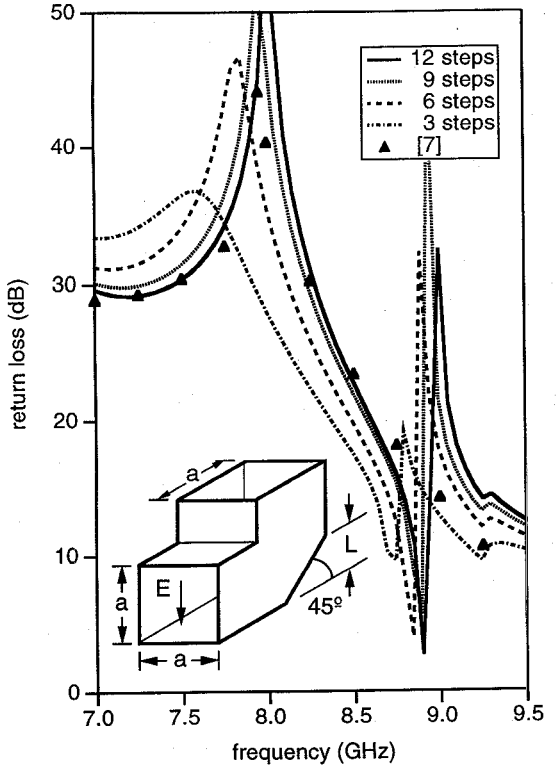

Fig. 3a TE_{10}-mode (E-plane) input return loss of mitered E-plane corner. Approximation of miter by increasing number of steps. Dimensions: a=22.86mm, L=17.78mm.

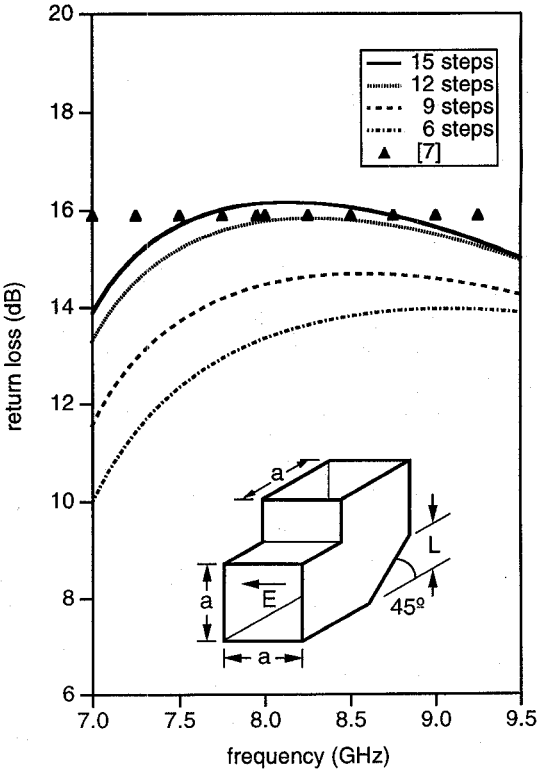

Fig. 3b TE_{01}-mode (H-plane) input return loss of mitered E-plane corner. Approximation of miter by increasing number of steps. Dimensions: a=22.86mm, L=17.78mm.

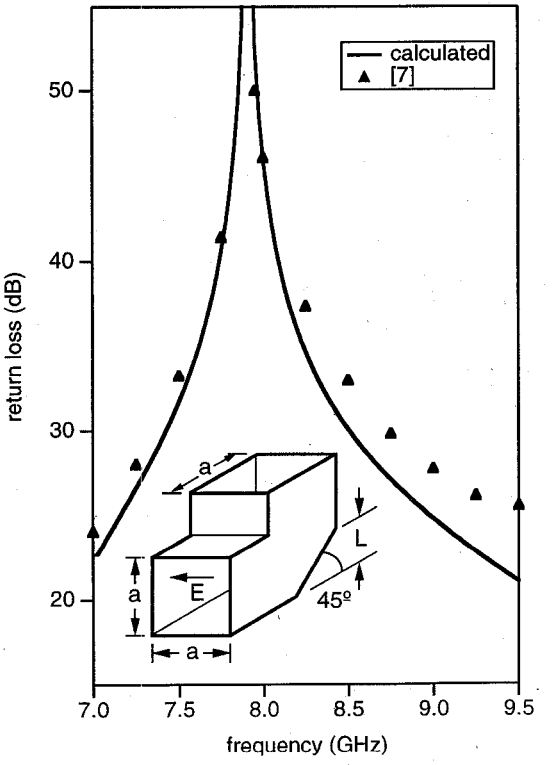

Fig. 4 Input return loss of H-plane corner with 22-step miter approximation. Dimensions: a=22.86mm, L=16.31mm.

parameters, becomes obvious when other components are connected to the structure in Fig. 1. Such an example is, for instance, the 180-degree bend shown in Fig. 5. Since the interactions of higher-order modes between the two 90-degree corners are rigorously taken into account, good agreement with the finite-element analysis [3] is obtained.

IV. CONCLUSION

A new generalized scattering matrix formulation of waveguide corners distorted by discontinuities is presented. Since the discontinuities in the resonator region are rigorously taken into account and their influences are transformed to the interfaces with the connected rectangular waveguides, the generalized scattering matrix - as opposed to hitherto known fundamental-mode parameters - of such structures can be calculated. The validity of this approach is demonstrated by comparison with measurements and a finite-element analysis at the examples of 90- and 180-degree waveguide bends.

REFERENCES

[1] E. Kühn, "A mode-matching method for solving field problems in waveguide and resonator circuits", *AEÜ*, Vol. 27, pp. 511-518, 1973.

[2] T. Sieverding and F. Arndt, "Field theoretic CAD of open or aperture matched T-junction coupled rectangular waveguide structures", *IEEE Trans. Microwave Theory Tech.*, vol. 40, pp. 353-362, Feb. 1992.

[3] J. Uher, J. Bornemann and U. Rosenberg, *Waveguide Components for Antenna Feed Systems. Theory and CAD*. Artech House Inc., Norwood 1993.

[4] P. Carle, "Right-Angle Junction for Rectangular Waveguide", in *21st European Microwave Conf. Proc.*, pp. 711-715, Sep.1991.

[5] X.-P. Liang, K.A. Zaki and A.E. Atia, "A rigorous three plane mode matching technique for characterizing waveguide T-junctions, and its application in multiplexer design", *IEEE Trans. Microwave Theory Tech.*, vol. 39, pp. 2138-2147, Dec. 1991.

[6] F. Alessandri, M. Mongiardo, R. Sorrentino, "Computer-aided design of beam forming networks for modern satellite antennas", *IEEE Trans. Microwave Theory Tech.*, Vol. 40, pp. 1117-1127, June 1992.

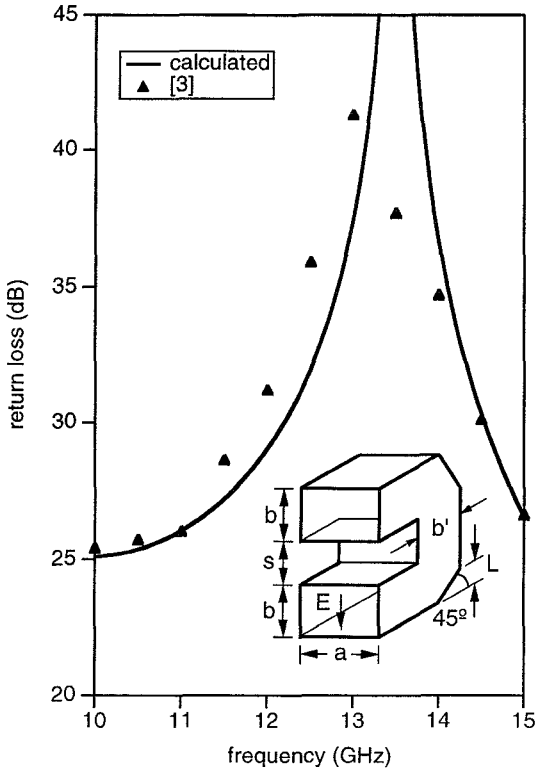

Fig. 5 Comparison of this theory (five-step miter approximation) with finite-element analysis [3] at a 180-degree E-plane bend. Dimensions: a=19.05mm, b=5.08mm, s=6.096mm, b'=4.826mm, L=4.167mm.

[7] P.K. Park, R.L. Eisenhart, and S.E. Bradshaw, "Matched dual mode square waveguide corner", in *1986 IEEE MTT-S Microwave Symp. Dig.*, pp. 155-156.

[8] J. Esteban and J.M. Rebollar, "Field theory CAD of septum OMT-polarizers", in *1992 APS Int. Symp. Dig.*, pp. 2146-2149.